Characterization of the On-Body Path Loss at 2.45 GHz and Energy Efficient WBAN Design for Dairy Cows

Said Benaissa, *Member*, *IEEE*, David Plets, *Member*, *IEEE*, Emmeric Tanghe, *Member*, *IEEE*, Günter Vermeeren, Luc Martens, *Member*, *IEEE*, Bart Sonck, Frank André Maurice Tuyttens, Leen Vandaele, Jeroen Hoebeke, Nobby Stevens, *Member*, *IEEE*, and Wout Joseph, *Senior Member*, *IEEE*

***Abstract*—Wireless Body Area Networks (WBANs) provide promising applications in the healthcare monitoring of dairy cows. The characterization of the path loss between on-body nodes constitutes an important step in the deployment of a WBAN. In this paper, the path loss between nodes placed on the body of a dairy cow was determined at 2.45 GHz. FDTD simulations with two half-wavelength dipoles placed 20 mm above a cow model were performed using a 3-D electromagnetic solver. Measurements were conducted on a live cow to validate the simulation results. Excellent agreement between measurements and simulations was achieved and the obtained path loss values as a function of the transmitter-receiver separation were well fitted by a lognormal path loss model with a path loss exponent of 3.1 and a path loss at reference distance (10 cm) of 44 dB. As an application, the packet error rate and the energy efficiency of different WBAN topologies for dairy cows (i.e., single-hop, multi-hop, and cooperative networks) were investigated. The analysis results revealed that exploiting multi-hop and cooperative communication schemes decreases the packet error rate and increases the optimal payload packet size. The analysis results revealed that exploiting multi-hop and cooperative communication schemes increases the optimal payload packet size and improves the energy efficiency by 30%.**

***Index Terms*—Cross-layer performance, dairy cow, energy efficiency, incremental cooperative relaying, multi-hop, on-body propagation, packet error rate, path loss, single-hop, wireless body area network (WBAN).**

I. Introduction

With the advances in wireless communication and micro-electro-mechanical systems (MEMS) [1], computing devices have become smaller and cheaper, together with increased functionality and higher energy efficiency. This combination makes it possible to build Wireless Body Area Networks (WBANs). The IEEE 802.15 Task Group 6 describes WBANs as "*low power devices operating in or around the human body (but not limited to humans) to serve a variety of applications including medical, consumer electronics /personal entertainment and other*" [2]. WBANs are finding various applications in the areas of medicine, agriculture, sports and multimedia [3], [4]. See [5] for a review of the application of WBANs for human health monitoring. By adopting this technology, doctors can remotely check the health status of the patients and they can recommend suitable medications. For example, prearrangement measurements can be taken to control many diseases such as high blood pressure, heart attack, diabetes, and cancer.

WBANs can be effectively used to track the health of dairy cows to enhance milk productivity and cow welfare, including detection of diseases such as lameness, a major health problem for dairy farming [6]. When cows are equipped with a WBAN, the farm manager can analyze multiple health parameters (e.g., temperature from the udder or ear) and activity information (e.g., movement from legs, position) in real time. The cow's health can be automatically assessed using a combination of these parameters.

Extensive studies on the modeling of on-body propagation loss for humans have been published [7], [4], [8]–[13] , but until now, no comparable studies have been done for dairy cows. This study is the first to propose a proper and efficient path loss model for on-body channel modeling for dairy cows, with the aim of helping to design and analyze the performance of such on-body sensor networks.

The goal of this work is to develop empirical on-body path loss models for dairy cows at 2.45 GHz using both simulations and experiments. We have also designed an energy efficient WBAN for dairy cows. The characterization of the propagation channel is necessary for efficient communication between the

S. Benaissa, D. Plets, E. Tanghe, G. Vermeeren, L. Martens, J. Hoebeke, and W. Joseph are with the Department of Information Technology, Ghent University/iMinds, Gaston Crommenlaan 8 Box 201, B-9050 Ghent, Belgium (e-mail: wout.joseph@intec.UGent.be).

S. Benaissa, B. Sonck, F.A.M. Tuyttens, and L. Vandaele are with the Institute for Agricultural and Fisheries Research (ILVO)-Animal Sciences Unit, Scheldeweg 68, 9090 Melle, Belgium (email: frank.tuyttens@ilvo.vlaanderen.be).

N. Stevens is with DraMCo research group, ESAT, Faculty of Engineering Technology, KU Leuven, Gebroeders De Smetstraat 1, 9000 Ghent, Belgium (email: nobby.stevens@kuleuven.be).

sensors placed at different parts of the cow's body. The 2.45 GHz band was selected because it is freely available and most of the practical existing technologies for WBANs work in this band. Here we propose a WBAN that monitors multiple health parameters: information collected from the hind and front leg, the udder, and the ear is forwarded to a data collector placed on the cow's neck. In practice, this node will forward all information to the data backend. Four on-body scenarios have been investigated, including both line-of sight (LOS) and non-LOS (NLOS) conditions. In addition to the path loss modeling, the cross-layer performances were investigated for different WBAN topologies, i.e., single-hop, multi-hop, and cooperative networks. Based on theoretical analysis and numerical simulations, the most optimal network architecture in terms of packet error rate and energy efficiency has been determined.

The following novelties are presented here: (i) experimental determination of the path loss for different on-body communication scenarios (i.e., ear to neck, hind leg to neck, front leg to neck, and udder to neck) based on measurements on a real cow using ZigBee motes, (ii) numerical investigation of the path loss of the same scenarios with simulations on a cow model using a 3-D electromagnetic solver (SEMCAD-X), and (iii) evaluation the packet error rate and the energy efficiency of three WBAN topologies for dairy cows using the proposed path loss models.

Below, Sections II-A and II-B present the measurement and simulation setup. Section II-C illustrates the investigated on-body communication scenarios. In Section II-D, the path loss model used to fit the obtained data is explained. Results of the path loss measurements and simulations are presented and discussed in Section III. In Section IV, the obtained path loss models are used to evaluate the packet error rate and the energy efficiency for different network topologies and conclusions are presented in Section V.

II. METHODS

A. Measurement Setup

1) Measurement environment and cow dimensions

Measurements were conducted in a state-of-the-art research barn at the Institute for Agricultural and Fisheries Research (ILVO) in Melle, Belgium. This barn, which houses approximately 144 lactating dairy cows, contains 2 milking robots, a conventional milking parlor, concentrate feeders and several features enabling experimental setups. On-body measurements were performed in a large area of about 6 m x 12 m, so that reflections from the walls can be ignored. One dairy cow was selected for the on-body measurements. The tested cow had the following dimensions: withers-tail 1.8 m, width 0.7 m, nose-tail 2.6 m, rump-hoof 1.4 m, stance (i.e., front-to-rear claws) 1.7 m, chest 0.8 m, withers (shoulder) height 1.4 m, and hook-bone width 0.6 m (Fig. 1-a).

2) On-body nodes

Path loss measurements were performed using two ZigBee motes. The transmitting ZigBee mote consists of an XBee S2 (XB24-Z7WIT-004) module with an omnidirectional monopole antenna (integrated whip, gain = 1.5 dBi). The receiving ZigBee mote is a RM090 module with an inverted F antenna (IFA, gain = 1 dBi). The receiving mote was attached to the cow's collar, which is the expected position of the sink node. After attachment, the antenna of the ZigBee mote was vertically polarized (with respect to the ground) with a separation of 20 mm above the cow's body. The same polarization and height were used for the transmitting antenna. The first ZigBee mote (TX) periodically transmits packets at 3 dBm power level and the other mote (RX) senses the *received signal strength indicator* (RSSI) information corresponding to the received packets and forwards this information to a laptop via USB interface (Fig. 1-b). Wireshark software was used to capture and analyze the packets received by the RX mote.

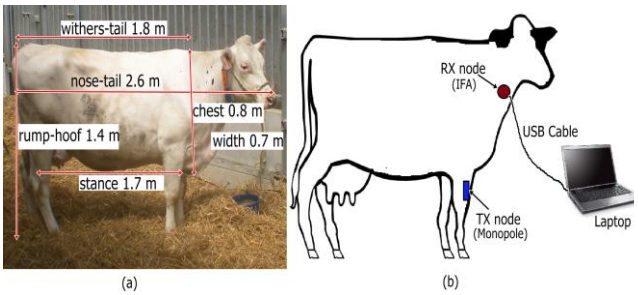

Fig. 1. (a) Cow dimensions and measurement environment and (b) on-body measurement setup.

3) RSSI calibration

The RSSI reported by the receiving ZigBee mote indicates the power level being received by the antenna (represented by a number). A calibration of the ZigBee mote using the spectrum analyzer has been done using experiments as in [14] to determine the relation between the RSSI and the radio-frequency (RF) power P_{RX}.

One ZigBee mote was configured as a coordinator, which broadcasts three packets per second (transmitter). Two receivers were used to sense the received power. The first receiver is another ZigBee mote configured as a sniffer to capture broadcast signals (ZigBee to ZigBee) and measure RSSI. The second receiver, comprised of a spectrum analyzer (R&S FSL6) connected to an MA431Z00 antenna (ZigBee to spectrum analyzer), was used to measure RF power. The antenna and ZigBee motes were placed 1 m above the ground. The sniffer was used to avoid acknowledgment packets, which can affect the received power of the spectrum analyzer. The distance between the transmitter and the receivers was increased by 0.5m steps, from 0.5 m to 12 m. For each separation between the transmitter and the receivers, 150 samples of the RF power measured by the spectrum analyzer and 150 RSSI samples reported by the ZigBee mote were logged using laptops. In order to account for the antenna gains and cable losses, the obtained samples were used to calculate the path loss (equation (1)) for the considered transmitter-receiver separations. Then, the path losses derived from the RSSI (ZigBee mote) and the RF power (spectrum analyzer) were fitted to plot path loss models (equation (4)).

Because the antennas were static and no objects were moving

in the subject's environment, the standard deviations over each of the 150 RSSI sample did not exceed 2 dB. The path loss models of the RSSI calibration were plotted in Fig 2. The path loss model (blue line) obtained from the RSSI values reported by the ZigBee mote was 8 dB higher than the path loss model obtained from the received power of the spectrum analyzer (dashed line). In addition, the path loss at the reference distance $PL(d_0 = 0.5\text{ m})$ was 36 dB for ZigBee-SA case. However, it shifted to 44 dB in the ZigBee-ZigBee scenario. The path loss exponents and the standard deviations were nearly the same for both path loss models. In conclusion, 8 dB will be added to the RSSI values reported by the ZigBee mote for the calibration to calculate the RF power values. Throughout the remainder of the paper, only actual RF powers will be mentioned.

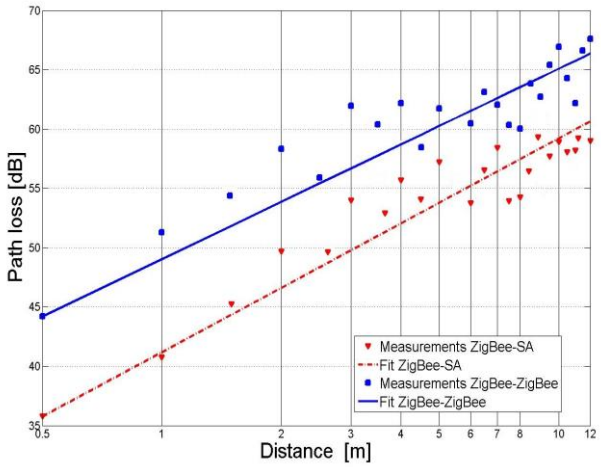

Fig. 2. RSSI calibration: measured path loss and fitted models versus distance (Tx-Rx separation). SA: spectrum analyzer.

B. Simulation Setup

Simulations were performed using the electromagnetic solver SEMCAD-X based on the finite-difference time domain (FDTD) computation method. This FDTD solver uses a non-uniform grid scheme. A maximum grid step of 2 mm was taken for the cow body model, which allows correct simulation of the frequency of 2.45 GHz [15].

For human body simulations, SEMCAD-X provides anatomically correct models of the human body [16]. No similar models exist for a cow's body, however, thus we developed a cow model with the same dimensions as the experimental cow. The authors of [17] explain that when studying the on-body radio channel at microwave frequencies, the internal composition of the human body does not play a major role because of the small value of the skin depth. Therefore, a homogeneous phantom made exclusively of muscle tissue is suitable for modelling on-body communication at 2.4 GHz [17]. Based on this conclusion, the cow body in our simulations was modeled as a homogeneous medium with the dielectric properties of cow muscle at 2.4 GHz, relative permittivity $\varepsilon_r = 52.791$ and conductivity $\sigma = 1.705$ S/m [18]. In order to account for the multipath effect, a ground with the electrical properties of the agricultural soil was added under the cow with a separation of 2 mm. As in [19], an electrical conductivity of 0.1 S/m and a relative permittivity of 3 were considered for the ground at 2.4 GHz. The multipath effect from the walls was negligible because the measurements were performed in a large area.

To model the transmitter and the receiver, two half-wavelength dipoles with length 56 mm and a realistic diameter of 1 mm were used. The receiving antenna was terminated by a load of 50 Ω. Both antennas were placed 20 mm above the cow phantom. Dipoles were used because they have a simple structure and they are the best understood antennas [11], [13]. Also, simulation of the cow phantom with the IFA and monopole antennas in the same SEMCAD-X model necessitates high memory capacity (IFA requires high resolution FDTD grading). Consequently, the grading size exceeds the memory capacity.

However, the antenna characteristics (e.g., antenna gain, radiation efficiency, and reflection coefficient) of the antennas used during measurements (monopole and IFA) near the cow's body are required for the path loss calculation (Section II-D). Therefore, each antenna (IFA and monopole) was simulated separately by the FDTD solver to compute its gain and efficiency in free space and near the cow's body.

For the transmitter, a simple quarter-wavelength monopole with a length of 30 mm was simulated. The receiver antenna consists of an IFA. The same antenna as [20] is designed and used for our simulations. The impedance of the IFA is matched directly to 50 Ω. Therefore no external matching components are needed. The antenna is implemented on a substrate with a thickness of 1 mm and a relative permittivity of $\varepsilon_r = 4.4$. Since there is no ground plane beneath the antenna, substrate thickness will have little effect on the performance [20].

C. Measurement and Simulation Scenarios

To design a WBAN that monitors multiple health parameters, different on-body wireless communication links have to be considered. Fig. 3 shows four scenarios where information from (i) hind leg (scenario I), (ii) udder (scenario II), (iii) leg front (scenario III), and (iv) the ear (scenario IV) is forwarded to the collector node RX placed on the cow's neck.

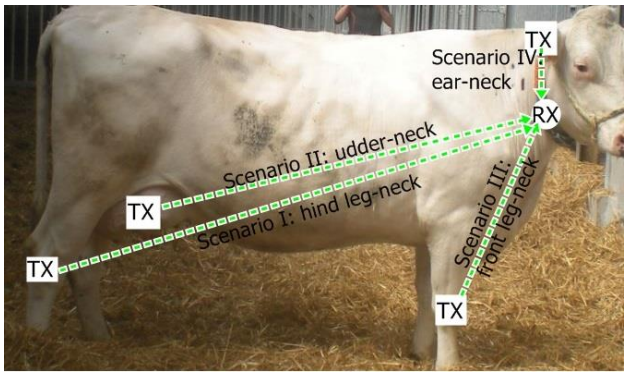

Fig. 3. On-body measurement and simulation scenarios.

Thirty-three positions were considered (Fig. 4): the RX mote was fixed on the collar of the cow, then the TX mote was placed at different distances from the neck. For the front and hind legs,

the TX was placed at the anterior and posterior sides of each leg. The test cow stood still during the measurements, and for each transmitter location *the average* of 150 RSSI values was considered. The receiving ZigBee mote was programmed to receive three RSSI values per second. The measurement results are compared to simulations performed with the FDTD solver (SEMCAD-X) at the same TX-RX positions as shown in Fig. 4.

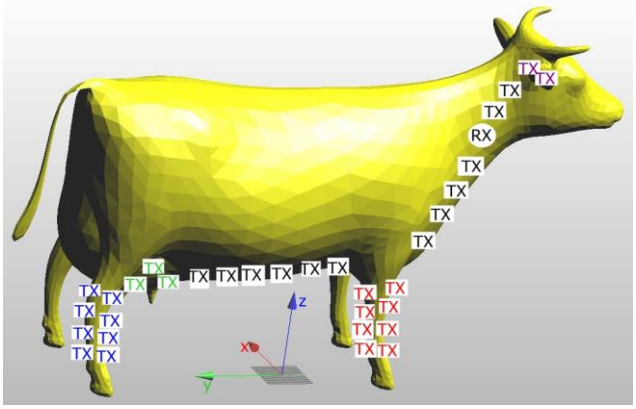

Fig. 4. On-body radio propagation measurement showing the receiver on the cow's neck while the transmitter is positioned at 33 locations on the body. RX, receiver; TX, transmitter. Each color represents the positions considered for each body part (i.e., blue: hind leg, green: udder, red: front leg, and purple: ear). The black positions are used for the whole body path loss calculation.

D. Path Loss Model

The received power P_{RX} is calculated from the RSSI values reported by the ZigBee mote after calibration (Section II.A-3). Then, the path loss (PL) is calculated as follows:

$$PL = P_{TX} + G_{TX} - L_{TX} + G_{RX} - L_{RX} - P_{RX} \quad (1)$$

where P_{TX} is the transmitter power (dBm), G_{TX} the transmitter antenna gain in *free space* (dBi), L_{TX} transmitter cable losses (dB), G_{RX} receiver antenna gain in *free space* (dBi), and L_{RX} the receiver cable losses (dB).

The definition of the path loss given by (1) cannot be applied immediately due to the inevitable interaction between the antennas and the cow's body. Because the antennas are positioned close to the cow's body, their characteristics (i.e., radiation pattern, gain) are influenced by the body charges. In this situation, the free space antenna gain cannot be used for calculating the path loss. In literature ([9], [11], [12], [17], [21]), the antenna gains are included in the WBAN path loss calculation given by (1). Thus the path loss, including the antenna gains as a part of the channel model (PL_{incl}), is calculated as follows:

$$PL_{incl} = P_{TX} - L_{TX} - L_{RX} - P_{RX} \quad (2)$$

However, with this approach, the obtained path loss models determined by simulations or measurements are specific for the antenna type used. To separate the antenna from the underlying channel, several new studies have tried to establish the so called "antenna de-embedding propagation models" [22]–[26].

In our study, the antenna gains near the body are calculated by FDTD simulations and used for the path loss calculation instead of the free space gains. Thus, the path loss PL excluding the antenna gains (i.e., antenna de-embedded path loss) is given by:

$$PL = P_{TX} + G_{TX\_b} - L_{TX} + G_{RX_b} - L_{RX} - P_{RX} \quad (3)$$

with G_{TX_b} and G_{RX_b} are the antenna gains of the transmitter and the receiver *near the cow's body* (at 20 mm, see above), respectively.

Similarly to [11] , a log-distance path loss model is proposed. The path loss can be modeled as a linear function of the logarithmic distance between the transmitter and receiver, as explained in [11]:

$$PL(d) = PL(d_0) + 10n\,log\left(\frac{d}{d_0}\right) + X_\sigma \quad (4)$$

with $PL(d_0)$ is the path loss at reference distance $d_0 = 10$ cm , n the path loss exponent, d the separation distance between TX and RX and X_σ a zero-mean Gaussian distributed variable (in dB) with standard deviation σ, also in dB.

III. Results and Discussion

A. Simulations: Antenna Characteristics

1) $|S_{11}|$ near the cow's body

The magnitude of the reflection coefficient in dB $|S_{11}|$ of an antenna determines the ability of the antenna to accept power from a source [27]. Lower values of $|S_{11}|$ indicate that the antenna reflects less power. The $|S_{11}|$ is derived from the input impedance of the antenna (Z_{in}). For maximum power transfer, Z_{in} should exactly match the output impedance of the source (e.g., 50 Ω). However, in real cases, the antenna presents an impedance mismatch.

The absolute value of the simulated reflection coefficient $|S_{11}|$ of the considered antennas (i.e., dipole, monopole, and IFA) in free space and near the cow's body is shown in Fig. 5, as a function of the frequency. It can be seen that $|S_{11}|$ under - 10 dB is achieved in the 2.45 GHz ISM band (2400-2483 MHz) [2]. Thus, each antenna shows good impedance matching. Moreover, based on Fig. 5, one can conclude that the input impedance of all antennas does not vary dramatically near the body in comparison to free space. This can be explained by the height of the antennas above the body (20 mm).

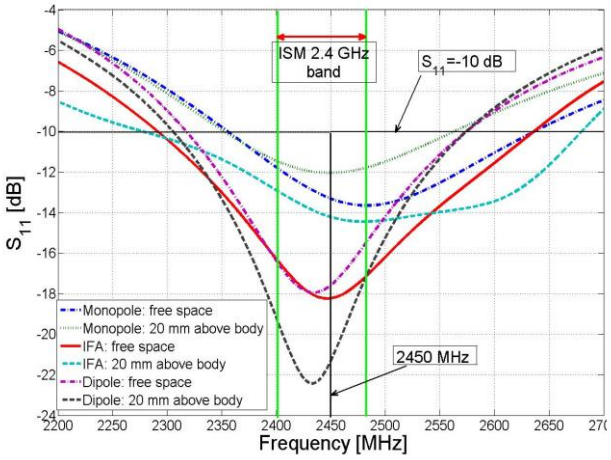

Fig. 5. Simulated $|S_{11}|$ of the dipole, monopole, and the inverted F antenna (IFA) in free space and near the cow's body (20 mm).

Table I lists the simulated $|S_{11}|$ at 2.45 GHz and the -10 dB bandwidth (BW) of the considered antennas. For the dipole antenna, the cow body makes the antenna reflect less power, indicated by the shift of $|S_{11}|$ from -17 dB in free space to -21 dB near the body. The $|S_{11}|$ decreases due to the decrease of the input antenna impedance (Z_{in}). For the dipole antenna, Z_{in} is closer to 50 Ω near the body in comparison to free space. However, due to the influence of the cow's body on the substrate, the IFA reflects more power close to the lossy medium. The $|S_{11}|$ of the monopole antenna is approximately the same in free space and near the body. The mismatch efficiency of each antenna is calculated from $|S_{11}|$. The values listed in Table I will be used to calculate the total efficiency.

Table I
Simulated $|S_{11}|$ at 2.45 GHz and the -10 dB bandwidth (BW) of the considered antennas.

		$\|S_{11}\|$ (2.45 GHz) [dB]	Mismatch efficiency [%]	-10 dB BW [MHz]
Dipole	Free space	-17.5	98	258
	Near body	-21.4	99	271
Monopole	Free space	-13.3	98	285
	Near body	-12.0	95	215
IFA	Free space	-18.1	98	346
	Near body	-14.2	96	400

2) Antenna gain and efficiency

The radiation efficiency of an antenna is defined as the ratio of total power radiated by the antenna to the net power accepted by the antenna from the connected source [28]. Table II lists the radiation efficiency of the dipole, monopole, and IFA in free space and near the cow's body. In free space, the antenna radiation efficiency varies from 86% for the IFA to 99% for the dipole and monopole antennas, indicating good radiation of the input power. The cow's body affects the radiation efficiency, however: the radiation efficiency near the cow's body decreases to between 85% (monopole) and 70% (dipole) in comparison to free space. Even so, this still indicates good radiation by the antennas near the body. In Table II, the total efficiency in free space and near the cow phantom is listed. This efficiency is the product of the mismatch efficiency (Table I) and the radiation efficiency (Table II). Since the mismatch efficiency is close to 100%, the total efficiency follows the same variation as the radiation efficiency. Table II lists also the simulated maximum antenna gain in dBi for the considered antennas in free space and 20 mm above the cow's body. In free space, the antenna gain ranges from 1.7 dBi for the monopole to 2.6 for the IFA. A typical value of 2.1 dBi is obtained for the dipole in free space. When the antennas are positioned near the cow's body, the gains increase and vary between 5.5 dBi for the dipole and 6.2 dBi for the IFA. We note that the maximum antenna gains are used for the path loss calculation given in equation (3). This is a good approximation for the path loss calculation, as the direction of the maximum gain is tangential to the cow's body. For the simulated path loss, the gain of the dipole near the cow's body is used. Due to the difficulty of measuring the antenna gains of the IFA and monopole near the body, the simulated gains (IFA near the neck and monopole near the udder, the ear, and the legs) are used for the calculation of the measured path loss (see equation (3)).

Table II
Dipole, monopole, and inverted F antenna (IFA) simulated gains and radiation efficiency (%) in free space and 20 mm above the cow's body at 2.45 GHz

		Gain [dBi]	Radiation efficiency [%]	Total efficiency [%]
Dipole	Free space	2.1	99	97
	Near neck	5.5	70	69
Monopole	Free space	1.7	99	94
	Near udder	5.3	85	83
IFA	Free space	2.6	86	84
	Near neck	6.2	74	70

B. Comparison and Validation: Measured versus Simulated Path Loss

1) Path loss values of the investigated on-body scenarios

Table III lists the average path loss values for the considered on-body wireless communication scenarios (i.e., ear-neck, hind leg-neck, front leg- neck, and udder-neck). For each body part, the positions mentioned in Fig. 4 are considered in the calculation of the average path loss. As explained in Section II.D (3), the path loss including (PL_{incl}) and excluding (PL) the antenna gains are calculated. Then the absolute deviations are computed as follows:

$$\delta_{incl} = \left|PL_{incl}^{meas} - PL_{incl}^{sim}\right| \quad (6)$$

$$\delta_{excl} = \left|PL^{meas} - PL^{sim}\right| \quad (7)$$

Where δ_{incl} and δ_{excl} are the absolute deviations between measurements and simulations when the antenna gains are included and excluded, respectively.

First, the measured path loss including the antenna gains (PL_{incl}^{meas}) varies between 53.4 dB for the scenario IV (i.e., ear-neck) and 69.7 dB for the scenario II (i.e., udder-neck). Scenario IV has the lowest value because of the short distance between the ear and the neck of the cow (about 50 cm). However, for scenario II (udder-neck), the cow's body obscures the communication between the udder and the neck, resulting in the highest path loss value. Scenarios I and III have approximately the same path loss values (63 dB). This result could be explained the similar influence that the legs (front and back) influence on the antennas. For the simulated path loss, PL_{incl}^{sim} varies between 51.0 dB (scenario IV) and 70.1 dB

Table III
Comparison between measured and simulated average path loss values for the investigated scenarios. δ_{incl} and δ_{excl} are the absolute deviations between measurements and simulations when the antenna gains are included and excluded, respectively.

Scenario	PL_{incl}^{meas} [dB]	PL_{incl}^{sim} [dB]	δ_{incl} [dB]	PL^{meas} [dB]	PL^{sim} [dB]	δ_{excl} [dB]
I- Hind leg-Neck	63.9	70.1	6.1	77.2	78.6	1.4
II- Udder-Neck	68.7	72.0	3.3	80.2	81.8	1.6
III- Front leg-Neck	62.2	65.7	3.4	74.0	76.3	2.3
VI- Ear-Neck	53.5	51.0	2.4	65.8	65.1	0.8
Average			3.8			1.6

(scenario II). The same discussion explains the measurement results. We also observed a difference of 3.8 to 6.1 dB between measurements and simulations indicated by the values of the absolute deviation δ_{incl} in Table III. These differences are expected because different antenna types were used during measurements (monopole and IFA) and simulations (dipoles).

After excluding the antenna gains (i.e., true path loss), we observed a decrease of the deviation between the measured and simulated path losses for all scenarios. In this case, the absolute deviation varies between 0.8 and 2.3 dB with an average of 1.6 dB. Thus, very good agreement between the measurements and the simulations was achieved, indicating that the obtained values can be used for the on-body path loss analysis of dairy cows.

2) Path loss model for the whole body

In order to develop a path loss model for the whole body, all positions shown in Fig. 4 were considered. For each transmitter-receiver separation, the average over the 150 RSSI samples was used to calculate the path loss values (the standard deviations over each 150 consecutive RSSI samples varied between 1 and 4 dB). Then, a least squares fit was performed (fit for measurements and fit for simulations) using the path loss values for the different transmitter-receiver distances to model the path loss as a linear function of the logarithmic distance. First, the obtained path loss models including the antenna gain (PL_{incl}) are shown in Fig. 6. The markers indicate the individual measurement and simulation samples, while the lines represent the path loss models obtained through the fitting of the data. For the individual samples (simulations and measurements), we distinguished between LOS and NLOS paths. As shown in Fig. 6, both measured and simulated LOS paths (e.g., neck to ear, neck to front leg) are associated with lower path loss values (most samples are under the fit line). However, NLOS paths (e.g., neck to udder) present high path loss values. For the same TX-RX separation, an average of 7 dB path loss difference was noticed between LOS and NLOS.

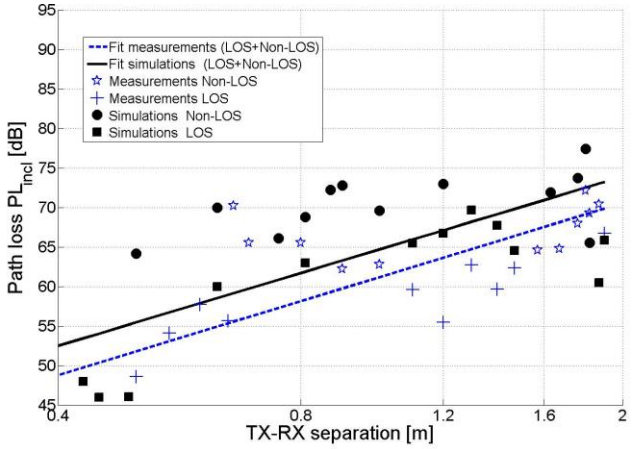

Fig. 6. Path loss models including the antenna gains (PL_{incl}) for the whole body (LOS: line-of-sight, NLOS: none-LOS)

The obtained path loss models excluding the antenna gain (PL) are shown in Fig. 7. The measured and simulated path loss models (PL), after excluding the antenna gains, show excellent correspondence (average deviation of less than 0.5 dB), which validates the results listed in Table III.

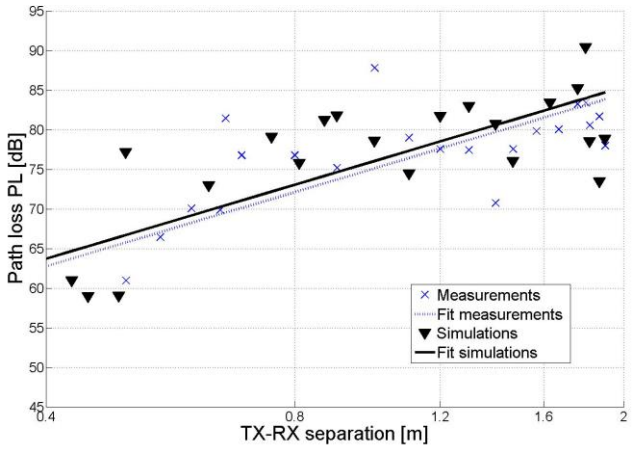

Fig. 7. Path loss models excluding the antenna gains (PL) for the whole body.

Table IV lists the values of path loss exponents and path loss at the reference distance obtained for the whole body. When the antenna gains are excluded, $PL(d_0)$ at reference distance ($d_0 = 10\ cm$) shifts from 30 to 44 dB for the measurement and from 34 to 45 dB for the simulations, while the path loss exponent remains the same ($n \approx 3.1$). To make a comparison with published works in the field (on-body for humans), we should consider the antenna-specific path loss models including the antenna gains (Fig. 6), as done in several studies [11]–[13], [21]. These studies have the limitation of being antenna-specific. The obtained results are comparable with the path loss models obtained for humans with respect to the body shape difference between humans and cows. In [12] for example, a path loss exponent of 3.11 and path loss at reference distance $PL(d_0 = 10\ cm)$ of 35 dB were obtained for line-of-sight (LOS) communications. In our measurements and simulations, both LOS and non-LOS (NLOS) communications (e.g., udder-neck) are considered. Nevertheless, the path loss values from the models shown in Fig. 6 are lower than those presented in [12]. This is due to the height of the antennas above the body (20 mm) in our study compared to 5 mm in [12] (more power absorption when the antenna is close to the body). Similar path loss models were found also in [21].

Table IV
Parameter values of the path loss models for the whole body.

	$d_0[cm]$	$PL(d_0)\ [dB]$	$n[-]$	$\sigma[dB]$	$R^2[-]$
PL_{incl}^{meas}	10	30	3.12	4.8	0.76
PL_{incl}^{sim}	10	34	3.06	6.4	0.71
PL^{meas}	10	44	3.15	4.9	0.79
PL^{sim}	10	45	3.11	5.5	0.78

The values of the standard deviation around the path loss model σ are also listed in Table IV. For simulation and measurement, standard deviations σ of 6 dB around the path loss model were observed due to the consideration of both LOS and NLOS conditions. The coefficient of determination R^2 measures how well the path loss model (regression line) approximates the real data points (measured or simulated path

losses). It is defined as the square of the correlation between the measured/simulated values and the predicted path losses [29]. As shown in Table IV, coefficients of determination greater than 0.7 were obtained in all path loss models, indicating a good fit of the obtained data with the log-normal path loss model.

IV. Application

Nodes in WBANs for dairy cows would use very small batteries with low processing and storage capabilities. Furthermore, such batteries would need to operate properly and autonomously for long periods of time without being recharged or replaced. For instance, the average lifetime of a cow is five years and most cows' anomalies (e.g., mastitis, heat, lameness) occur after the first calving (around second year). This means that the healthcare monitoring system should operate at least three years without needing to be charged. Energy consumption is therefore an important issue in a WBAN deployment for dairy cows. Several choices that can impact energy consumption, e.g., sample transmit rate, complexity of routing algorithms, applications (node's data rate), and programming languages [30]. To reduce the energy consumption and maintenance requirements associated with recharging of batteries, an efficient network topology can be a crucial factor for extending battery lifetime [31].

In general, a WBAN topology comprises a set of sensor nodes and a sink node. In traditional WBAN topologies, each sensor collects information about the cow and sends it to the sink. This is known as *single-hop* communication. However, the sensor can also send the information through *multi-hop* links, where special devices, called relay nodes or relays, can be added to the WBAN to collect all the information from sensors and send it to the sink, thus improving the WBAN lifetime and reliability [12], [31]–[33]. Furthermore, recent work attempts to justify the use of *cooperative* communications in a WBAN, by exploiting diversity gain achieved via cooperation among the relay nodes [34]. Moreover, cooperative communication represents a potential candidate to suppress the channel fading effects in WBANs.

In this section, we evaluate the packet error rate (*PER*) and the energy efficiency as a function of the transmit power and packet payload for communication between the udder and the neck of the cow using the three WBAN communication schemes (i.e., single-hop, two-hop, and cooperative communication). The obtained path loss models (Section V) and the energy consumption of available commercial radios (i.e., ZL70101 and nRF24L01) are being considered [35], [36]. The goal is to investigate which topology is the most suitable for a dairy cow WBAN in terms of PER and energy efficiency. To the best of our knowledge, this has not yet been done for dairy cow WBANs.

A. Communication Schemes

Here we investigate three communication schemes (Fig. 8). The automatic repeat request (ARQ) protocol (i.e., acknowledgement messages are sent by the receiver, indicating that it has correctly received a data frame or packet) is implemented at the link layer to improve reliability.

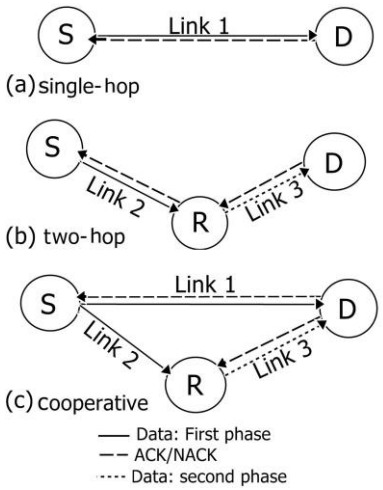

Fig. 8. Investigated communication schemes: (a) single-hop, (b) two-hop, and (c) cooperative network. S=Source, R=Relay, and D=Destination.

The first scheme consists of a single-hop communication (i.e., direct communication) between the source (S) and the destination (D) nodes (Fig. 8 (a)). The second scheme uses one relay R in a two-hop topology (Fig. 8 (b)). Compared with a single-hop, a two-hop network may suffer more packet losses due to the use of multiple radio links. Also, the source should separate between relays and destination acknowledgement messages. Therefore, a simple ARQ cannot be directly applied in this case. In [37], local end-to-end relay ARQ (LE RARQ) is proposed to avoid redundant retransmissions by the source node. This protocol is used for our analysis of a two-hop network topology (Fig. 8 (b)). In the first phase, S sends the data packet to R. If R receives the data correctly, the packet is relayed to D in a second phase. Then, an acknowledgment (ACK) message is sent to R and then to S. If the data is corrupted at the relay level, a negative relay ACK (NRACK) is sent to S. If the data is corrupted at the destination level, a negative ACK is sent to R and then to S, indicating that the link 3 (Fig. 8 (b)) fails and that link 2 is reliable. The retransmission will be done then by R only. Thus, the power consumption of S can be reduced. The third investigated communication scheme is shown in Fig. 8 (c). Conventional cooperative relaying wastes the wireless channel because the relays always forward the signals regardless of the channel conditions [38]. To overcome this limitation, incremental relaying schemes were proposed to save channel resources by adapting the relaying process to the channel conditions. This approach is explained in [34]. The ARQ used in the cooperative scheme is similar to two-hop. The unique difference is that the destination node in a cooperative scheme can receive the packet at the first phase. However, in a two-hop scheme, the packet is received first by the relay node and then forwarded to the destination.

B. Packet Error Rate

In our analysis of the packet error rate and the energy efficiency, we considered a cow WBAN in which the link between two nodes is affected by propagation loss, shadowing, and additive white Gaussian noise (AWGN). Then a differential binary phase shift keying (DBPSK) modulation is used, as

recommended by IEEE 802.15.6 [2].

The bit error rate BER for coherently detected, differentially encoded BPSK is theoretically given by [39]:

$$BER = \text{erfc}\left(\sqrt{\frac{E_b}{N_0}}\right)\left(1 - 0.5erfc\left(\sqrt{\frac{E_b}{N_0}}\right)\right) \quad (8)$$

where erfc is the error function, E_b the energy per bit [J], and N_0 the noise power spectral density [W/Hz]. Next, E_b/N_0 is calculated from the signal to noise ratio (SNR) at the receiver level as follows:

$$\frac{E_b}{N_0} = SNR.\frac{B_N}{R_d} \quad (9)$$

Here, B_N is the noise power bandwidth (Hz); R_d is the data rate of the sensor node (bits/sec). The effective isotropically radiated power (EIRP) of the node can be calculated as:

$$EIRP = P_{TX} + \eta_{dB} \quad (10)$$

with P_{TX} as defined in (1) and $\eta_{dB}$is the total antenna efficiency [dB]. The *SNR* at the receiver level is expressed in decibels (dB) as:

$$SNR_{dB} = EIRP - PL(d) - P_N \quad (11)$$

with P_N being the AWGN power [dBm] and $SNR = 10^{(SNR_{dB}/10)}$.

After the calculation of the BER, the packet error rate can be derived for each communication scheme using the packet size N (expressed in bits). Assuming that the bit errors are independent, the PER_{SH} of a single-hop transmission is computed as [40]:

$$PER_{SH} = PER_{SD} = 1 - (1 - BER)^N \quad (12)$$

where PER_{SD} is the packet error rate of the link source (S) to destination (D). For a two-hop case, a packet error occurs when one of the following events happens: (i) the S-R link fails or (ii) the S-R link is error free and the R-D link fails. Hence the packet error rate PER_{TH} for a two-hop case is computed as follows:

$$PER_{TH} = PER_{SR} + PER_{RD}(1 - PER_{SR}) \quad (13)$$

With PER_{SR} is the PER of the source S-R link and PER_{RD} is the PER of the R-D link. Based on [34], the PER of the single-stage decode and forward incremental cooperative relaying scheme PER_C is given by:

$$PER_C = PER_{SD}PER_{SR} + PER_{SD}(1 - PER_{SR})PER_{RD} \quad (14)$$

C. Energy Efficiency

To determine the overall energy consumption, we take the transmit power P_{TX} [W], the circuit energy consumption at the transmitter E_{TX_elec} [nj/bit] and at the receiver E_{RX_elec} [nj/bit] for both data as well as ACK/NACK packets into account. In our analysis of the energy consumption, we adopt the energy models proposed in [34], [38], [40], [41]. To differentiate between data and ACK/NACK packets, we consider L the number of bits of a data packet, A the number of bits of an ACK/NACK packet, and H the header size.

For a single-hop scheme, the overall energy consumption per bit is simply the energy per bit consumed by the transmitter (electronic + transmission $=E_{TX\_elec} + \frac{P_{TX}}{R_d}$) and the receiver ($E_{RX\_elec}$). Then we multiply by the number of bits per packet (data or ACK/NACK) to obtain the total energy consumption per packet. Hence, for a data packet:

$$E_{SH\_DATA} = \left(E_{TX\_elec} + E_{RX\_elec} + \frac{P_{TX}}{R_d}\right)(L + H) = x(L + H) \quad (15)$$

where $x = E_{TX\_elec} + E_{RX\_elec} + \frac{P_{TX}}{R_d}$. Similarly, the energy consumed during the transmission of an ACK/NACK packet is given by:

$$E_{SH\_ACK/NACK} = x(A + H) \quad (16)$$

The energy efficiency is defined as the ratio of useful part of energy consumed to the total energy consumed in a communication link between sender and receiver. Thus, for the single-hop scheme, the energy efficiency η_{SH} is determined as follows [34]:

$$\eta_{SH} = \frac{(1 - PER_{SH})xL}{E_{SH\_DATA} + E_{SH\_ACK/NACK}} \quad (17)$$

The energy efficiency for a two-hop scheme is derived considering the following events for a successful transmission of a data packet:

(a) A successful communication for both S-R and R-D links, consumes $2E_{TX\_elec} + 2E_{RX\_elec} + 2\frac{P_{TX}}{R_d}$ per bit. This event occurs with a probability with $(1 - PER_{SR})(1 - PER_{RD})$.

(b) The S-R link is error free and the R-D link fails occurs with a probability $(1 - PER_{SR})PER_{RD}$. The same energy as (a) is consumed.

(c) The link S-R fails with a probability PER_{SR}. No transmission between R and D is made. Therefore, the consumed energy is $E_{TX\_elec} + E_{RX\_elec} + \frac{P_{TX}}{R_d}$. The total energy to successfully transmit a data packet E_{TH_DATA} can be computed as follows:

$$E_{TH_{DATA}} = \begin{bmatrix} \left(2E_{TX_{elec}} + 2E_{RX_{elec}} + 2\frac{P_{TX}}{R_d}\right)(1 - PER_{SR}) \\ + \left(E_{TX_{elec}} + E_{RX_{elec}} + \frac{P_{TX}}{R_d}\right)PER_{SR} \end{bmatrix}(L + H) \quad (18)$$

Similarly, for an ACK/NACK packet, the total consumed power is given by:

$$E_{TH\_ACK/NACK} = [2x(1 - PER_{SR}) + xPER_{SR}](A + H) \quad (19)$$

Consequently, the energy efficiency for two-hop scheme η_{TH} can be calculated as:

$$\eta_{TH} = \frac{(1 - PER_{TH})xL}{E_{TH\_DATA} + E_{TH\_ACK/NACK}} \quad (20)$$

For the cooperative scheme, we adopt the calculations made in [34]. The total energy consumption involved in the transmission of a data packet E_{C_DATA} and ACK/NACK packet $E_{C\_ACK/NACK}$ using cooperative communication with incremental relaying is given as follows [34]:

$$E_{C_{DATA}} = \begin{bmatrix} \left(E_{TX_{elec}} + 2E_{RX_{elec}} + \frac{P_{TX}}{R_d}\right)(1 - PER_{SD}) \\ + \left(E_{TX_{elec}} + 2E_{RX_{elec}} + \frac{P_{TX}}{R_d}\right) PER_{SD} PER_{SR} \\ + \left(E_{TX_{elec}} + 2E_{RX_{elec}} + \frac{P_{TX}}{R_d}\right) PER_{SD}(1 - PER_{SR}) \end{bmatrix} (L + H) \quad (21)$$

$$E_{C\_ACK/NACK} = \left[\left(E_{TX_{elec}} + 2E_{RX_{elec}} + \frac{P_{TX}}{R_d}\right)\left(1 + PER_{SD}(1 - PER_{SR})\right)\right]_{(A+H)} \quad (22)$$

Thus, the energy efficiency for the cooperative scheme η_C can be computed as:

$$\eta_C = \frac{(1 - PER_C)xL}{E_{C\_DATA} + E_{C\_ACK/NACK}} \quad (23)$$

D. Scenario

We consider a scenario where communication is performed between the udder (source) and the neck (destination) (see Fig. 3). As shown in Section III, this scenario presents the highest path loss value (Table II). Therefore, a relay node is used to forward the information of the source to the destination. We propose using the sensor node placed on the front leg as a relay node. In this way, no new nodes are introduced to the cow WBAN illustrated in Fig. 3. The goal is to evaluate the PER as a function of the transmit power and the packet payload of the sensor node. Then we determine the optimal network topology in terms of the packet error rate and the energy efficiency.

Table V lists the parameters used for the PER and the energy efficiency analysis. The on-body channel model for a cow WBAN obtained from measurements (including the antenna gains) was adopted. Because the measured path loss is used, the antenna efficiency of the monopole is also used (i.e., transmitter). The symbols are transmitted with a typical data rate of 250 kbps. The energy consumption of the ZL70101 and the nRF24L01 of commercial radios is considered [35], [36]. A noise power of -90 dBm is used for the PER and energy efficiency analysis, based on the measurement of the noise power conducted inside the barn. The other parameters are listed in Table V.

Table V
Parameter values used for on-body dairy cow WBAN packet error rate and energy efficiency analysis.

Parameter		Value	Unit
On–body	d_0	10	cm
Channel model	$PL(d_0)$	30	dB
	n	3.12	[-]
	X_σ	4.8	dB
Noise power		-90	dBm
Antenna efficiency		76	%
Data rate		250	kbps
Packet size		128	Bytes
Overhead size		80	bits
ACK/NACK size		64	bits
R_d/B_N		0.25	bps/Hz
E_{TX_elec}		11.25	nJ/bit
E_{RX_elec}		11.25	nJ/bit

E. Results and Discussion

1) Packet Error Rate

The packet error rate is shown (Fig. 9) as a function of the transmit power for the considered network topologies. Here, the packet size is fixed to 128 bytes as recommended by IEEE 802.15.6 [2]. We observe that the cooperative scheme presents the lower PER (highest performance) whereas the single-hop presents the highest PER. In addition, for a transmit power lower than -6 dBm the two-hop gives the same PER as the cooperative. For instance, to ensure a PER of 10^{-4}, a transmit power of -5 dBm for the cooperative and two-hop schemes, and -2 dBm for single-hop is required. Thus, the relaying communication, either by cooperation or multi-hop, uses low power to give the same performance (PER) as the single-hop. This allows the battery lifetime of the cow sensor nodes to be extended for long-term health and welfare monitoring. It is important to note that the relaying process requires additional nodes, thus increasing the network cost.

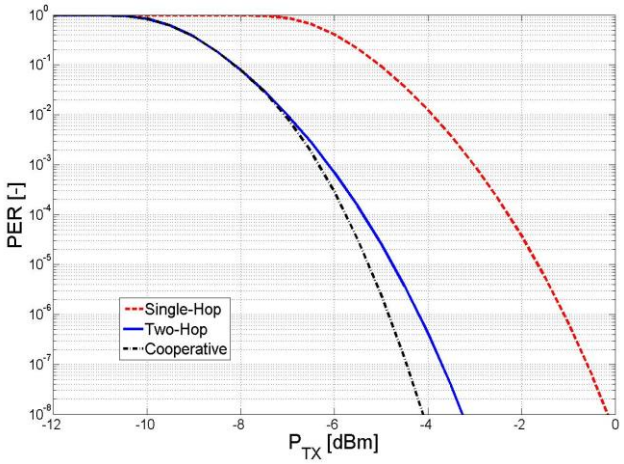

Fig. 9. PER as a function of the transmit power [dBm] for the investigated communication schemes (packet size 128 bytes).

2) Energy efficiency

In Fig. 10, energy efficiency is shown as a function of the sensors' transmit power for a packet size of 128 bytes. As shown in Fig. 10, a threshold transmit power exists that separates a region where a single-hop network topology is better from a region where relaying schemes (cooperation or multi-hop) are useful for energy efficiency. We clearly observe that the single-hop scenario is the most energy efficient network (80%) when the transmit power exceeds -2 dBm. Further, the single-hop scheme is twice as efficient as the two-hop scheme (40%). Keeping in mind that the sensor nodes in the cow's WBAN are designed to work with low power values to extend the battery lifetime, the cooperative and two-hop scenarios present an energy efficiency larger than the single-hop scheme. For example, a transmit power of -6 dBm ensures an energy efficiency of 40% and 35% for two-hop and cooperative communications, respectively. However, energy efficiency is

even less than 10% in the single-hop case.

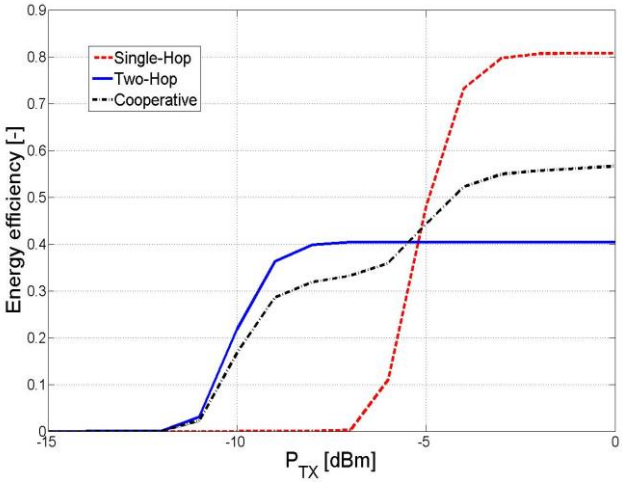

Fig. 10. Energy efficiency as a function of the transmit power [dBm] for the investigated communication schemes (packet size 128 bytes).

To determine the optimal packet payload that maximizes the energy efficiency for the investigated network topologies, Fig. 11 depicts the energy efficiency for different packet sizes (i.e., from 10 to 3000 bits). We note that all the investigated network topologies are inefficient when the transmit power is lower than -10 dBm. With a transmit power of -5 dBm, no optimal packet payload exists for a two-hop scheme. However, the optimal packet sizes that maximize the energy efficiency for the single-hop and cooperative topologies are 550 bits (energy efficiency 50%) and 960 bits (energy efficiency 40%), respectively. In fact, this is a trade-off between energy efficiency and packet size. In the case of -10 dBm, an optimal packet size exists for cooperative and two-hop communications, with approximately the same value (500 bits). However, the energy efficiency is less than 25%. For single-hop communication, energy efficiency is negligibly small, and optimal behavior is not observed. For transmit powers higher than 0 dBm, no optimal packet size is present in all investigated schemes. We note that for a two-hop network, the energy efficiency is the same when transmit powers of -5 and 0 dBm are used (Fig. 10). Therefore, the curves of the energy efficiency as a function of the payload coincide (Fig. 11).

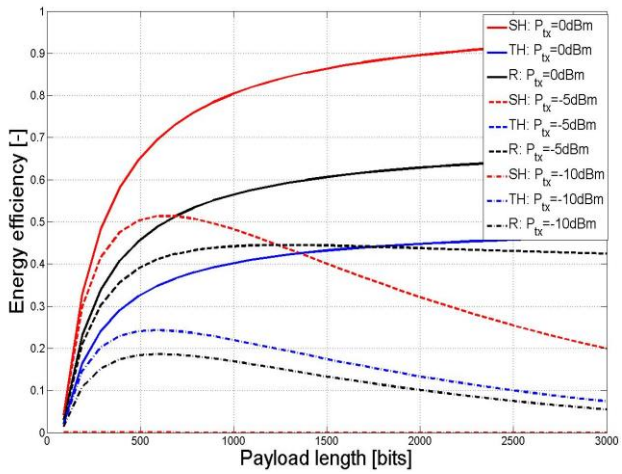

Fig. 11. Energy efficiency as a function of the payload length for a transmit power P_{TX}=0dBm, P_{TX}=-5dBm, and -10dBm. SH=single-hop, TH=two-hop, C=cooperative.

Based on the results presented is this section, WBANs for dairy cows can be realized in practice. These networks should include a combination of single-hop, multi-hop, and cooperative topologies.

V. Conclusion and Future Work

In this paper, the propagation path loss for different on-body wireless communications links of a dairy cow (ear to neck, hind leg to neck, front leg to neck, and udder to neck) has been characterized by both measurements and simulations. Measurements on a dairy cow in a multipath environment (barn) have been performed to validate the simulations conducted using a cow body phantom. The path loss values obtained from the simulations show good agreement with the values derived from the measurements. The udder to neck and ear to neck scenarios presented the highest and the lowest path loss values with an average of 81 dB and 65 dB, respectively. In addition, a log-normal path loss model has been constructed from measurement and simulation data for the whole cow's body. Excellent agreement has been achieved between the measured and the simulated path loss models with a path loss exponent of 3.1 and a path loss at reference distance (10 cm) of 44 dB.

The physical propagation analysis has been used to investigate the performances of the cross-layer of a cow-WBAN single-hop, multi-hop, and cooperative based network. The packet error rate and the energy efficiency have been derived as a function of the sensor node transmit power and the payload length. By using a relay node placed on the front leg of the cow, multi-hop and cooperative communications have allowed higher performances than the single-hop communication in terms of power consumption, optimal packet size, and energy efficiency.

Communication in WBANs is mostly challenged by cow movements or posture changes. Therefore, investigation of further channel parameters such as delay spread and fast fading (dynamic channel) for an accurate on-body wireless channel characterization will be one of the next steps of the work. Further, an extension to ultra-wideband (UWB) channel measurements will be an interesting topic for future work. Other possible future research could include the forward error correction (FEC) block codes and the packet retransmission when evaluating the packet error rate and energy efficiency.

Acknowledgments

This work was supported by the iMinds-MoniCow project, co-funded by iMinds, a research institute founded by the Flemish Government in 2004, and the involved companies and institutions. E. Tanghe is a Postdoctoral Fellow of the FWO-V (Research Foundation – Flanders). The authors would like to thank Thijs Decroos, Sara Van Lembergen, Leen Verloock, and Matthias Van den Bossche for their help during the measurements.

REFERENCES

[1] J. M. Kahn, R. H. Katz, and K. S. J. Pister, "Emerging Challenges: Mobile Networking for Smart Dust," *J. Commun. Networks*, vol. 2, no. 3, pp. 188–196, 2000.

[2] 802.15 Working Group, "IEEE Standard for local and metropolitan area networks part 15.6: Wireless Body Area Networks: IEEE Std 802.15. 6-2012," *Doc. is available IEEE Xplore*, no. February, 2012.

[3] I. Khemapech, I. Duncan, and A. Miller, "A survey of wireless sensor networks technology," *6th Annu. Postgrad. Symp. Converg. Telecommun. Netw. Broadcast.*, vol. 6, p. 6, 2005.

[4] Y. Hao, A. Alomainy, P. S. Hall, Y. I. Nechayev, C. G. Parini, and C. C. Constantinou, "Antennas and propagation for body centric wireless communications," in *2005 IEEE/ACES International Conference on Wireless Communications and Applied Computational Electromagnetics*, 2005, vol. 2005, pp. 588–591.

[5] J. Ahmad and F. Zafar, "Review of Body Area Network Technology & Wireless Medical Monitoring," *Int. J. Inf. Commun. Technol. Res.*, vol. 2, no. 2, pp. 186–188, 2012.

[6] L. D. Warnick, D. Janssen, C. L. Guard, and Y. T. Gröhn, "The effect of lameness on milk production in dairy cows.," *J. Dairy Sci.*, vol. 84, no. 9, pp. 1988–1997, 2001.

[7] Q. H. Abbasi, A. Sani, A. Alomainy, and Y. Hao, "Numerical characterization and modeling of subject-specific ultrawideband body-centric radio channels and systems for healthcare applications," *IEEE Trans. Inf. Technol. Biomed.*, vol. 16, no. 2, pp. 221–227, 2012.

[8] A. Alomainy, Y. Hao, A. Owadally, C. G. Parini, Y. Nechayev, C. C. Constantinou, and P. S. Hall, "Statistical Analysis and Performance Evaluation for On-Body Radio Propagation With Microstrip Patch Antennas," *IEEE Trans. Antennas Propag.*, vol. 55, no. 1, pp. 245–248, 2007.

[9] P. S. Hall, Y. Hao, Y. I. Nechayev, A. Alomalny, C. C. Constantinou, C. Parini, M. R. Kamarudin, T. Z. Salim, D. T. M. Hee, R. Dubrovka, A. S. Owadally, W. Song, A. Serra, P. Nepa, M. Gallo, and M. Bozzetti, "Antennas and propagation for on-body communication systems," *IEEE Antennas Propag. Mag.*, vol. 49, no. 3, pp. 41–58, 2007.

[10] M. Khan, Q. Abbasi, and R. Ashique, "Comprehensive Design and Propagation Study of a Compact Dual Band Antenna for Healthcare Applications," *J. Sens. Actuator Networks*, vol. 4, no. 2, pp. 50–66, 2015.

[11] E. Reusens, W. Joseph, and G. Vermeeren, "On-body measurements and characterization of wireless communication channel for arm and torso of human," *Microw. Symp. Dig. 2008 IEEE MTT-S Int.*, pp. 903–906, 2007.

[12] E. Reusens, W. Joseph, B. Latre, B. Braem, G. Vermeeren, E. Tanghe, L. Martens, I. Moerman, and C. Blondia, "Characterization of On-Body Communication Channel and Energy Efficient Topology Design for Wireless Body Area Networks," *Inf. Technol. Biomed. IEEE Trans.*, vol. 13, no. 6, pp. 933–945, 2009.

[13] L. Roelens, W. Joseph, E. Reusens, G. Vermeeren, and L. Martens, "Characterization of scattering parameters near a flat phantom for wireless body area networks," *IEEE Trans. Electromagn. Compat.*, vol. 50, no. 1, pp. 185–193, 2008.

[14] D. Plets, W. Joseph, K. Vanhecke, E. Tanghe, and L. Martens, "Coverage prediction and optimization algorithms for indoor environments," *EURASIP Journal on Wireless Communications and Networking*, vol. 2012, no. 1. p. 123, 2012.

[15] J. B. Schneider, "Understanding the Finite-Difference Time-Domain Method," *Self Publ.*, 2013.

[16] M. J. Ackerman, "The visible human Project: A resource for anatomical visualization," in *Studies in Health Technology and Informatics*, 1998, vol. 52, pp. 1030–1032.

[17] P. S. Hall and Y. Hao, *Antennas and Propagation for Body-Centric Wireless Communications. Second Edition*, 2nd ed. Norwood, MA, USA: Artech House, Inc., 2012.

[18] S. Gabriel, R. W. Lau, and C. Gabriel, "The dielectric properties of biological tissues: III. Parametric models for the dielectric spectrum of tissues.," *Phys. Med. Biol.*, vol. 41, no. 11, pp. 2271–2293, 1996.

[19] H. T. Anastassiu, S. Vougioukas, T. Fronimos, C. Regen, L. Petrou, M. Zude, and J. Käthner, "A computational model for path loss in wireless sensor networks in orchard environments," *Sensors (Switzerland)*, vol. 14, no. 3, pp. 5118–5135, 2014.

[20] A. Andersen, "Texas Instruments: Design Note 007 - 2.4 GHz Inverted F Antenna," 2008.

[21] M. M. Khan, Q. H. Abbasi, A. Alomainy, and C. Parini, "Experimental Investigation of Subject-Specific On-Body Radio Propagation Channels for Body-Centric Wireless Communications," *Electronics*, vol. 3, no. 1, pp. 26–42, 2014.

[22] M. Grimm and D. Manteuffel, "Antennas and Propagation for On- , Off- and In-Body Communications," 2013.

[23] M. Grimm and D. Manteuffel, "Electromagnetic wave propagation on human trunk models excited by half-wavelength dipoles," *2010 Loughbrgh. Antennas Propag. Conf. LAPC 2010*, no. November, pp. 493–496, 2010.

[24] M. Grimm and D. Manteuffel, "Evaluation of the Norton equations for the development of body-centric propagation models," *Proc. 6th Eur. Conf. Antennas Propagation, EuCAP 2012*, pp. 311–315, 2012.

[25] J. Naganawa, M. Kim, T. Aoyagi, and J. Takada, "FDTD-based Antenna De-embedding in WBAN on-body Channel Modeling," *2014 Xxxith Ursi Gen. Assem. Sci. Symp. (Ursi Gass)*, vol. 3, no. 2, p. 25008831, 2014.

[26] D. Kurup, W. Joseph, E. Tanghe, G. Vermeeren, and L. Martens, "Extraction of Antenna Gain From Path Loss Model for in-Body Communication," *Electron. Lett.*, vol. 47, no. 23, pp. 1262–1263, 2011.

[27] T. S. Bird, "Definition and misuse of return loss," *IEEE Antennas and Propagation Magazine*, vol. 51, no. 2, pp. 166–167, 2009.

[28] Propagation Committee, Antenna Standards Society, "IEEE standard definitions of terms for antennas," 1969.

[29] D. Wang, L. Song, X. Kong, and Z. Zhang, "Near-ground path loss measurements and modeling for wireless sensor networks at 2.4 GHz," *Int. J. Distrib. Sens. Networks*, vol. 2012, 2012.

[30] S. Lee and M. Annavaram, "Wireless Body Area Networks: Where does energy go?," in *2012 IEEE International Symposium on Workload Characterization (IISWC)*, 2012, pp. 25–35.

[31] W. Joseph, B. Braem, E. Reusens, B. Latre, L. Martens, I. Moerman, and C. Blondia, "Design of Energy Efficient Topologies for Wireless On-Body Channel," *Wirel. Conf. 2011-Sustainable Wirel. Technol. (European Wireless), 11th Eur.*, vol. 5, no. 4, pp. 1–7, 2011.

[32] A. Ehyaie, M. Hashemi, and P. Khadivi, "Using relay network to increase life time in wireless body area sensor networks," in *IEEE International Symposium on a World of Wireless, Mobile, and Multimedia Networks & Workshops*, 2009, pp. 1–6.

[33] J. Elias, "Optimal design of energy-efficient and cost-effective wireless body area networks," *Ad Hoc Networks*, vol. 13, no. PART B, pp. 560–574, 2014.

[34] K. S. Deepak and A. V Babu, "Improving energy efficiency of incremental relay based cooperative communications in wireless body area networks," *Int. J. Commun. Syst.*, vol. 28, no. 1, pp. 91–111, 2015.

[35] "Zarlink ZL70101. Datasheet at: http://www.zarlink.com/zarlink/." .

[36] "Nordic nRF24L01+. Datasheet at: http://www.nordicsemi.com/."

[37] T. M. Lin, W. T. Chen, and S. L. Tsao, "An efficient automatic repeat request mechanism for wireless multihop relay networks," *IEEE Trans. Veh. Technol.*, vol. 62, no. 6, pp. 2830–2839, 2013.

[38] A. K. Sadek, W. Yu, and K. J. R. Liu, "On the energy efficiency of cooperative communications in wireless sensor networks," *ACM Trans. Sens. Networks*, vol. 6, no. 1, pp. 1–21, 2009.

[39] B. Sklar, *Digital communications: fundamentals and applications*. 2001.

[40] M. C. Domingo, "Packet Size Optimization for Improving the Energy Efficiency in Body Sensor Networks," *ETRI J.*, vol. 33, no. 3, pp. 299–309, 2011.

[41] Z. Zhou, S. Member, and S. Zhou, "Energy-Efficient Cooperative Communication in a Clustered Wireless Sensor Network," *IEEE Trans. Veh. Technol.*, vol. 57, no. 6, pp. 3618–3628, 2008.